

SIMULATION OF A SOLAR HYBRID ABSORPTION/THERMOCHEMICAL REFRIGERATION SYSTEM FOR A RESIDENTIAL APPLICATION

Fitó de la Cruz, Jaume⁽¹⁾; Mauran, Sylvain^(2,3);

Stitou, Driss⁽²⁾; Mazet, Nathalie⁽²⁾; Coronas, Alberto⁽¹⁾

jaume.fito@estudiants.urv.cat

⁽¹⁾Universitat Rovira i Virgili, CREVER, Department of Mechanical Engineering

⁽²⁾PROMES-CNRS, Laboratoire Procédés, Matériaux et Energie Solaire

⁽³⁾Université de Perpignan Via Domitia (UPVD)

ABSTRACT

Further improvement of solar refrigeration systems depends strongly on development of more efficient energy storage systems. A hybrid absorption / thermochemical refrigeration system is proposed in this work, where both subsystems share the same condenser, evaporator and refrigerant fluid, making the overall system more economic and better performing than operating both parts separately. Performance of the system is evaluated by means of a simulation in a sample scenario, consisting of a demand of refrigeration for a single-family residence. The influence of varying the number of solar thermal collectors and the mass of refrigerant fluid available for storage at the thermochemical subsystem is studied.

Keywords: Solar refrigeration, thermochemical storage, hybrid systems.

1. Introduction

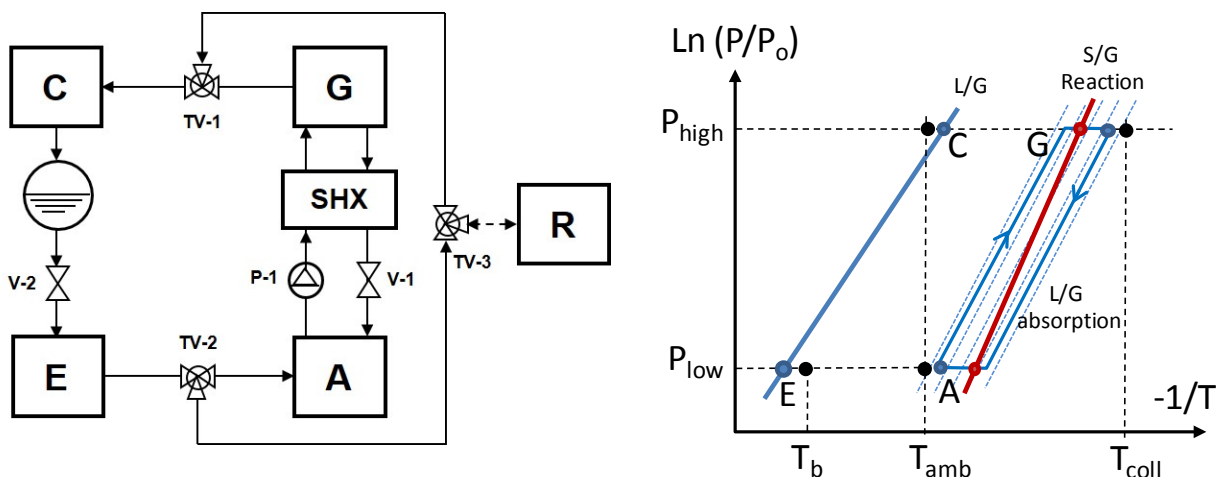
Efficient solar systems need to cope with the mismatch between the available solar radiation and the demand of energy. Sensible heat storage is a common solution [1], but it is not very energetic efficient.

Thermochemical systems are a promising option for solar applications [2]. As well as viability for refrigeration applications, they intrinsically offer high-density energy storage (thus reducing the system's size) with virtually no losses, for long periods of time [3-5], although they show low COP values (due to issues about solid-phase heat transfer). It is interesting to combine a thermochemical storage system with a refrigeration cycle with higher COP, for instancesolar absorption refrigeration cycles, which have been investigated [6].

In this work, a new solar hybrid absorption/thermochemical cycle is proposed and described, in a more economic and better performing design than just driving both systems separately.

2. Cycle description

The proposed cycle is shown in Fig. 1. Its configuration is similar to a conventional absorption cycle, but with an added reactor (R) for the thermochemical subcycle. Both the thermochemical and the absorption subcycles can share the same condenser (C) and evaporator (E) only if they use the same fluid as refrigerant. Selecting the same refrigerant (F) for both subsystems is the most practical



decision, since the global system becomes economic and compact.

Fig. 1. Hybrid absorption / thermochemical cycle.

The global system can be operated continuously even when there is no heat source available, as long as there is enough energy stored by the thermochemical subsystem. The connection $R \leftrightarrow TV-3$ is showed as a dashed line to indicate that the stream in it can flow in either direction, depending on the mode (charge or discharge) in which the subsystem is operating.

The absorption subsystem works the same way as a conventional absorption chiller. The generator (G) receives heat (Q_G) from the solar collector to regenerate the sorbent. Refrigerant vapor condenses at the condenser, rejecting condensation heat (Q_C). The regenerated sorbent goes to the absorber (A), to absorb the refrigerant vapor and release absorption heat (Q_A). In the evaporator, the refrigerant evaporates, removing heat (Q_E), being this the useful effect of the refrigeration cycle. The solution heat exchanger (SHX) improves the system's overall efficiency.

The thermochemical subsystem [7] is formed by the condenser (C), the evaporator (E) and a reactor (R) in which occurs a solid/gas reaction written in its generic form as:



with $\langle \text{MX} \rangle$ being a solid reactive salt having fixed μ or $(\mu + \nu)$ moles of gas (F) per mole of salt. Note that the stoichiometric coefficient μ may be zero.

The two salts $\langle \text{MX} \cdot \mu \text{F} \rangle$ and $\langle \text{MX} \cdot (\mu + \nu) \text{F} \rangle$, and the vapor (F) constitute a monovariant system, i.e. at a given pressure, fixed by the condenser or the evaporator, the equilibrium temperature of the reaction is fixed whatever the mole proportion of the two salts. That is a first great difference with the absorption system, which is bivariant.

Moreover the transformation of reactor is intrinsically non-stationary, the composition of the reactive salt evolving between $\langle \text{MX} \cdot \mu \text{F} \rangle$ and $\langle \text{MX} \cdot (\mu + \nu) \text{F} \rangle$. The sense of the reaction depends on the constraint temperature applied to the reactor at a given pressure. For a constraint temperature lower than the equilibrium one, the reaction evolves from left to right in the expression (1). In this case, the reaction is exothermic and the heat released at the constraint temperature is $\nu \cdot \Delta h_r$ for one mole of salt. Inversely for a higher temperature than the equilibrium one, the reaction evolves from right to left and is endothermic.

3. Performance indicators

Performance assessment is a common and important issue when evaluating a system's potential, and especially when comparing it with other systems. In this work, following indicators are proposed for the cycle: Coefficient Of Performance (COP), and Coefficient of Satisfaction of the Demand (CSD).

3.1. Coefficient Of Performance (COP)

The COP of the system for a determined operation period was defined as the relation between the total useful refrigeration effect delivered at the evaporator and the total driving heat input to the cycle (pump work being neglected), as it can be seen in (2).

$$COP^\xi = \frac{\int_{t=t_0^\xi}^{t=t_n^\xi} \dot{Q}_E^\xi(t) \cdot dt}{\int_{t=t_0^\xi}^{t=t_n^\xi} \dot{Q}_{in}^\xi(t) \cdot dt} \quad \{\xi = [HYB, ABS, TCH]\} \quad (2)$$

This definition of COP deals in terms of energy instead of power, because of the intermittent operation of this system. The values t_0^ξ and t_n^ξ correspond to the integration time limits for each subsystem. The term \dot{Q}_{in}^ξ corresponds to the driving heat input to the cycle under consideration: for the absorption subcycle (ABS), it is the heat input to the generator, \dot{Q}_G ; for the thermochemical subcycle (TCH), it is the heat input to the reactor, \dot{Q}_R ; and for the global hybrid system (HYB), it is the sum of these two. The term \dot{Q}_E^ξ corresponds to the useful refrigeration effect provided by the cycle under consideration.

3.2. Coefficient of Satisfaction of the Demand (CSD)

Although the COP shows performance by comparing the useful output to the heat input, it is also interesting to compare the output to the energy need in the application. A specific performance indicator, the Coefficient for Satisfaction of the Demand (CSD), is proposed for this system (3).

$$CSD^\xi = \frac{Q_{need} - \int_{t=t_0^\xi}^{t=t_n^\xi} \frac{[\dot{Q}_{need}(t) - \dot{Q}_E^\xi(t)]^2}{\dot{Q}_{need}(t)} dt}{Q_{need}} \quad \{\xi = [HYB, ABS]\} \quad (3)$$

with $Q_{need} \left(= \int_{t=t_0^\xi}^{t=t_n^\xi} \dot{Q}_{need}(t) \cdot dt \right)$ the cooling effect needed for the application.

According to this definition, it results that $0 \leq CSD \leq 1$. If the cooling effect provided by the system ($\dot{Q}_E^\xi(t)$) equals the demand ($\dot{Q}_{need}(t)$), then $CSD = 1$. If the cooling effect is zero, then $CSD = 0$.

4. System's performance preliminary simulation

Two main steps can be distinguished in the simulation procedure: estimation of a sample energy demand profile, and calculation of the cycle's operation.

4.1. Definition of the demand profile

To show the strengths of the cycle proposed in this work, the demand of cooling for a sample residence has been estimated on an hourly basis. Hypotheses and parameters concerning the residence can be seen in Table 1.

Table 1. Assumed parameters for estimation of demand profile.

Location	Barcelona
Date	July
Building type	Single-family residence
Building floor area (m ²)	100
Monthly demand of cooling (MWh)	0.85
Base temperature for cooling (°C)	21

The hourly demand of cooling was estimated through the degrees day method. This method has been proven to obtain very close-to-reality results among the simple methods [8], due to the considerable effect of the external environment temperature on the thermal demand.

According to this method, the monthly demand is expressed as a function of the specific monthly demand, $q_{need,m}$ (reference values available from real measurements, specialized bibliography or simulation software [9]), and the residence's floor area (A_{floor}), and then normalized through the cooling degree days (CDD_m , CDD_d). CDD (4-5) are a function of the hourly ambient temperature ($T_{amb,h}$) and the base temperature for cooling (T_b). A hourly utilization factor (α_h), a redistribution factor (k_d) and a weekend factor (β_{we}) were used to make hourly calculations for working days ($Q_{need,wd,h}$) (6) and weekends ($Q_{need,we,h}$) (7). Demand was assumed to be 50% higher during weekends [10].

$$CDD_m = \frac{\sum_{h=1}^{h=m} (T_{amb,h} - T_b)}{24} \quad \text{for } T_{amb,h} > T_b \quad (4)$$

$$CDD_d = \frac{\sum_{h=1}^{h=d} (T_{amb,h} - T_b)}{24} \quad \text{for } T_{amb,h} > T_b \quad (5)$$

$$Q_{need,wd,h} = \alpha_h \cdot k_d \cdot q_{need,m} \cdot A_{floor} \cdot \frac{CDD_{wd}}{CDD_m} \quad (6)$$

$$Q_{need,we,h} = \alpha_h \cdot k_d \cdot \beta_{we} \cdot q_{need,m} \cdot A_{floor} \cdot \frac{CDD_{we}}{CDD_m} \quad (7)$$

4.2. Model equations

The simulation scenario was conceived as the hybrid cycle being connected to a solar thermal system (see Table 2), and satisfying the cooling demand of a residence.

Information about hourly ambient temperature and solar radiation for the selected location was processed to obtain the hourly solar radiation on the collector field ($\dot{Q}_{rad}(t)$). With this value and having into account the global efficiency of the solar thermal system (η_{solar}), the hourly total driving heat input ($\dot{Q}_{in}(t)$) was determined (8).

$$\dot{Q}_{in}(t) = \dot{Q}_{rad}(t) \cdot \eta_{solar} \quad (8)$$

Then, calculations for each subcycle were made. Main temperatures for the absorption subcycle are presented in Table 2.

Table 2. Assumed parameters for the solar thermal collectors and the absorption subsystem.

Solar collector parameters		Absorption subsystem temperatures	
Solar collector type	Flat plate	Generator temperature, T_G ($^{\circ}\text{C}$)	90
Collector slope	45°	Condenser temperature, T_C ($^{\circ}\text{C}$)	35
Useful area of one collector (m^2)	2.3624	Evaporator temperature, T_E ($^{\circ}\text{C}$)	5
Solar thermal system efficiency (η_{solar})	0.5	Absorber temperature, T_A ($^{\circ}\text{C}$)	35

For the absorption subcycle, two cases are considered when calculating the driving heat input to the generator, depending on whether or not the absorption part alone can satisfy the whole demand (9 or 10, respectively).

$$\dot{Q}_G(t) = \frac{\dot{Q}_{need}(t)}{COP^{ABS}} \quad \text{if} \quad \dot{Q}_{in}(t) \cdot COP^{ABS} \geq \dot{Q}_{need}(t) \quad (9)$$

$$\dot{Q}_G(t) = \dot{Q}_{in}(t) \quad \text{if} \quad \dot{Q}_{in}(t) \cdot COP^{ABS} < \dot{Q}_{need}(t) \quad (10)$$

Once the heat input to the generator is known, calculation of the useful cooling effect delivered at the evaporator by the absorption subcycle is straightforward (11).

$$\dot{Q}_E^{ABS}(t) = \dot{Q}_G(t) \cdot COP^{ABS} \quad (11)$$

Surplus heat produced by the solar system is derived to the thermochemical subcycle (12), causing some refrigerant to vaporize due to the reaction (13) and therefore storing some cooling capacity in form of liquefied refrigerant (14), which can be later utilized. When calculating the amount of refrigerant being vaporized at the reactor, a value is needed for the enthalpy of reaction (Δh_r); for reactions involving ammonia, a standard value of 40 kJ/(mole of NH_3) can be assumed as an approximation. Since all the demand is covered by the absorption subcycle in this period, no cooling effect needs to be provided by the thermochemical subcycle (15).

$$\dot{Q}_R(t) = \dot{Q}_{in}(t) - \dot{Q}_G(t) \quad \text{if} \quad \dot{Q}_{in}(t) \cdot COP^{ABS} > \dot{Q}_{need}(t) \quad (12)$$

$$\dot{m}_r^{TCH}(t) = \frac{\dot{Q}_R(t)}{\Delta h_r} \quad \text{if} \quad \dot{Q}_{in}(t) \cdot COP^{ABS} > \dot{Q}_{need}(t) \quad (13)$$

$$m_r^{TCH}(t) = m_r^{TCH}(t-1) + \dot{m}_r^{TCH}(t) \cdot \Delta t \quad \text{if} \quad \dot{Q}_{in}(t) \cdot COP^{ABS} > \dot{Q}_{need}(t) \quad (14)$$

$$\dot{Q}_E^{TCH}(t) = 0 \quad \text{if} \quad \dot{Q}_{in}(t) \cdot COP^{ABS} > \dot{Q}_{need}(t) \quad (15)$$

The other way around, when the absorption subcycle alone cannot satisfy the demand, some cooling effect has to be provided by the thermochemical part (16). Some of the stored refrigerant is vaporized (17), being therefore destored (18), and also rejecting heat at the reactor (19).

$$\dot{Q}_E^{TCH}(t) = \dot{Q}_{need}(t) - \dot{Q}_E^{ABS}(t) \quad \text{if} \quad \dot{Q}_{in}(t) \cdot COP^{ABS} < \dot{Q}_{need}(t) \quad (16)$$

$$\dot{m}_r^{TCH}(t) = \frac{\dot{Q}_E^{TCH}(t)}{\Delta h_v} \quad \text{if} \quad \dot{Q}_{in}(t) \cdot COP^{ABS} < \dot{Q}_{need}(t) \quad (17)$$

$$m_r^{TCH}(t) = m_r^{TCH}(t-1) - \dot{m}_r^{TCH}(t) \cdot \Delta t \quad \text{if} \quad \dot{Q}_{in}(t) \cdot COP^{ABS} < \dot{Q}_{need}(t) \quad (18)$$

$$\dot{Q}_R(t) = \frac{\dot{Q}_E^{TCH}(T)}{COP^{TCH}} \quad \text{if} \quad \dot{Q}_{in}(t) \cdot COP^{ABS} < \dot{Q}_{need}(t) \quad (19)$$

For periods where the absorption subcycle can provide exactly the amount of cold demanded, $\dot{Q}_R(t)$, $\dot{Q}_E^{TCH}(t)$ and $\dot{m}_r^{TCH}(t)$ become zero. In any case, it must be always verified that the total useful cooling effect delivered at the evaporator is the sum of that of the absorption part and that of the thermochemical part (20). In case the system is not designed to cover 100% of the demand, an auxiliary heat source is needed (21).

$$\dot{Q}_E^{HYB}(t) = \dot{Q}_E^{ABS}(t) + \dot{Q}_E^{TCH}(t) \quad (20)$$

$$\dot{Q}_E^{TOT}(t) = \dot{Q}_E^{HYB}(t) + \dot{Q}_E^{AUX}(t) \quad (21)$$

The absorption subcycle is assumed to operate always when possible, due to its higher COP. When it cannot satisfy the demand alone, the thermochemical subsystem operates. Any surplus of driving heat will be stored by means of the thermochemical subcycle.

Calculations were carried out considering different working pairs, which can be seen in Table 4, and different number of solar thermal collectors in the residence.

Table 4. Working pairs considered for the simulations.

Option	Absorption subsystem	Thermochemical subsystem
A	H ₂ O / LiBr	H ₂ O / SrBr
B	NH ₃ / LiNO ₃	NH ₃ / BaCl ₂
C	NH ₃ / NaSCN	NH ₃ / BaCl ₂

Properties of ammonia have been obtained from [11]. Properties of water have been obtained from [12]. Correlations from [13] have been used for calculation of H₂O+LiBr properties. Vapour pressure data for NH₃+LiNO₃ were provided by [14], and data for density and isobaric specific heat are available in [15]. Regarding the mixture NH₃+NaSCN, data from [16] are used for vapour pressure, density and isobaric specific heat. Correlations from [17] have been used for specific enthalpy of NH₃+LiNO₃ as well as NH₃+NaSCN. A program has been developed with Engineering Equation Solver (EES) software which contains all properties correlations as internal functions. A fixed COP of 0.3 was assumed for the thermochemical subsystem.

5. Simulation results and discussions

Fig. 2a shows the variation of hybrid system's COP with varying number of solar thermal collectors, from one to ten. As expected, COP decreases with increasing number of collectors, from a value near to the absorption subsystem's COP when only one collector is installed, to a decreasing value a little bit closer to the thermochemical subsystem's COP with every additional collector. Since the COP for the thermochemical subsystem is lower than that of the absorption subsystem, and amount of surplus energy to be stored increases with every additional collector, the decrease in COP is logical, since the subsystem with lower COP gains more presence in the operation. Similar effect occurs when more mass of refrigerant is available for storage at the thermochemical subsystem. Essentially, the COP of the hybrid system decreases whenever more driving heat is provided to the thermochemical subsystem (either by increasing the number of collectors or the available mass of refrigerant for storage).

It can also be observed that the decrease in the COP is greater when a small number of collectors are being used, while the value remains almost flat after certain number of collectors. Profiles show that the COP is also dependent on the working pair under use and the mass of refrigerant available for storage.

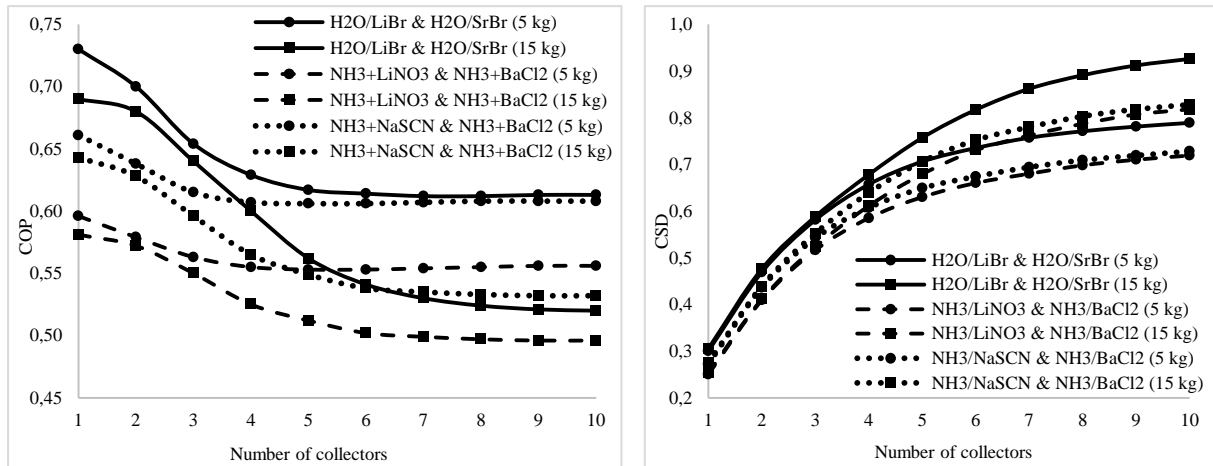


Fig. 2. Effect of number of solar thermal collectors on hybrid system's performance for different working pairs and mass of refrigerant (in kg) available for storage. (a) Evolution of COP. (b) Evolution of CSD.

Fig. 2b shows the variation of hybrid system's CSD with varying number of solar thermal collectors, from one to ten. As expected, its value increases with increasing number of collectors, since higher fraction of refrigeration needs can be covered by the system. Similar to COP, the mass of refrigerant for storage in the thermochemical subsystem has an appreciable impact. In this case, however, the working pair under use in the absorption subsystem has not as big impact on CSD values as on COP values. The reason is simple: increasing the CSD depends mainly on the performance of the thermochemical subsystem, not the absorption one. Last, but not least, it can also be observed that for a small number of collectors, CSD is very similar in all cases under consideration.

6. Conclusions

In this work, a new configuration for a hybrid absorption / thermochemical refrigeration system is proposed for solar applications. A definition of COP in terms of energy instead of power is proposed for its performance evaluation, and in addition, a new indicator named CSD is proposed to evaluate how well the system can satisfy the demand. A sample profile of refrigeration demand for a residence is built through the degrees day method, and a simplified model is described to carry out a preliminary simulation of the system in that sample case. Results indicate that increasing the amount of driving heat provided to the thermochemical subsystem (either by installing more solar thermal collectors or by allowing more mass of refrigerant to be stored) leads to a decrease in the hybrid system's COP and, in exchange, an increase in the CSD. This means that it is possible for this system to cover the demand even when solar radiation is not available, but by reducing its performance.

7. References

- [1] Pinel P., Cruickshank C. A., Beausoleil-Morrison I., Wills A. (2011). A review of available methods for seasonal storage of solar thermal energy in residential applications. *Renewable and Sustainable Energy Reviews* 15, 3341-3359.
- [2] Mette B., Kerskes H., Drück H. (2012). Concepts of long-term thermochemical energy storage for solar thermal applications – Selected examples. *Energy Procedia* 30, 321-330.
- [3] Cot-Gores, J., Castell, A., Cabeza, L. F. (2012). Thermochemical energy storage and conversion: A-state-of-the-art review of the experimental research under practical conditions. *Renewable and Sustainable Energy Reviews*, 16(7), 5207–5224.
- [4] Mauran, S., Lahmidi, H., Goetz, V. (2008). Solar heating and cooling by a thermochemical process. First experiments of a prototype storing 60kWh by a solid/gas reaction. *Solar Energy*, 82(7), 623–636.

- [5] Kerskes, H., Mette, B., Bertsch, F., Asenbeck, S., Drück, H. (2012). Chemical energy storage using reversible solid/gas-reactions (CWS) – results of the research project. *Energy Procedia* 30, 294-304.
- [6] Kim, D. S., & Infante Ferreira, C. A. (2008). Solar refrigeration options - a state-of-the-art review. *International Journal of Refrigeration* 31(1), 3–15.
- [7] Lahmidi H., Mauran S., Goetz V. (2006). Definition, test and simulation of a thermochemical storage process adapted to solar thermal systems. *Solar Energy* 80, 883-893.
- [8] Heller, A. (2000). Demand modelling for central heating systems. Report R-040, Department of Buildings and Energy. Technical University of Denmark (DTU). ISBN: 87-7877-042-4.
- [9] Pedersen, L. (2007). Load modelling of buildings in mixed energy distribution systems [dissertation]. Trondheim, Norway: Norwegian University of Science and Technology NTNU; 2007.
- [10] López Villada, J. Integración de sistemas de refrigeración solar en redes de distrito de frío y de calor [dissertation]. Tarragona, Spain: Universitat Rovira i Virgili, 2010.
- [11] Tillner-Roth R., Harms-Watzenberg F., Baehr H.D. (1993). Eine neue Fundamentalgleichung für Ammoniak. *DKV-Tagungsbericht* 20, 167-181.
- [12] Harr L., Gallagher J.S., Kell G.S., NBS/NRC Steam Tables, Hemisphere Publishing Corp., 1984.
- [13] Patek J. & Klomfar J. (2006). A computationally effective formulation of the thermodynamic properties of LiBr-H₂O from 273 to 500 K over full composition range. *Int. J. of Refrigeration* 29, 566-578.
- [14] Libotean S., Salavera D., Valles M., Esteve X., Coronas A. (2007). Vapor-Liquid Equilibrium of Ammonia + Lithium Nitrate + Water and Ammonia + Lithium Nitrate Solutions from (293.15 to 353.15) K. *J. Chem. Eng. Data* 52, 1050-1055.
- [15] Libotean S., Martín A., Salavera D., Valles M., Esteve X., Coronas A. (2008). Densities, Viscosities, and Heat Capacities of Ammonia + Lithium Nitrate and Ammonia + Lithium Nitrate + Water Solutions between (293.15 and 353.15) K. *J. Chem. Eng. Data* 53, 2383-2388.
- [16] Chaudhari S. K., Salavera D., Coronas A. (2011). Densities, Viscosities, Heat Capacities, and Vapor-Liquid Equilibria of Ammonia + Sodium Thiocyanate Solutions at Several Temperatures. *J. Chem. Eng. Data* 56, 2861-2869.
- [17] Farshi L.G., Infante Ferreira C.A., Mahmoudi S.M.S., Rosen M.A. (2014). First and second law analysis of ammonia/salt absorption refrigeration systems. *International Journal of Refrigeration* 40, 111-121.